Applied Physics Letters ARTICLE pubs.aip.org/aip/apl

Optoelectronic oscillator based on a silicon microring modulator

Cite as: Appl. Phys. Lett. **125**, 071104 (2024); doi: 10.1063/5.0213446
Submitted: 10 April 2024 · Accepted: 27 July 2024 ·
Published Online: 12 August 2024

Xiang Li,[1] Jia Xu Brian Sia,[2] Jiawei Wang,[2] Zhongliang Qiao,[3] Wanjun Wang,[2] Xin Guo,[2] Hong Wang,[2,a)] and Chongyang Liu[4,a)]

AFFILIATIONS

[1]Shenzhen Pinghu Laboratory, 2 Laolang Road, Shenzhen 518111, China
[2]School of Electrical and Electronic Engineering, Nanyang Technological University, 50 Nanyang Avenue, 639798 Singapore
[3]Key Laboratory of Laser Technology and Optoelectronic Functional Materials of Hainan Province, and School of Physics and Electronic Engineering, Hainan Normal University, No. 99 Longkun Road, Haikou 571158, China
[4]Temasek Laboratories, Nanyang Technological University, 50 Nanyang Drive, 637553 Singapore

[a)]**Authors to whom correspondence should be addressed:** ewanghong@ntu.edu.sg and liucy@ntu.edu.sg

ABSTRACT

An optoelectronic oscillator (OEO) system is built up with a high-speed silicon microring modulator. The modulator is based on a p-n doped ring resonator with a radius of 10 μm. Its electro-optic (EO) 3 dB bandwidth is ~31.7 GHz, which makes it suitable for generating multi-GHz radio frequency signals. By using this modulator, one of the essential components of an OEO, the EO converter, has been dramatically miniaturized. At the same time, assisted by the ring resonator, the phase noise of the generated 10 GHz signal (nearly −90 dBc/Hz at 10 kHz offset) is not compromised compared to other integrated OEOs with mm footprint modulators. This is an important step toward a compact, scalable, and fully integrated silicon photonics-based OEO system together with our existing integrated light sources and photodetectors.

Spectrally pure radio frequency (RF) or microwave signals in the frequency range of megahertz to hundreds of gigahertz have a variety of applications ranging from metrology, communications, sensing, to defense-related applications such as radar.[1–3] Conventional electronic oscillators, based on, for example, piezoelectric quartz resonators, are particularly suitable for intrinsic generation of such signals, but only at low frequencies (below 100 MHz) as high Q factor is only available in this range, and phase noise of the signal is directly related to the Q factor of the resonators.[3] Signals in the GHz range can be obtained by multiplying the intrinsic megahertz output from electronic oscillators. However, when the pure signal is multiplied toward gigahertz, the noise will also be amplified. As a result, the phase noise performance of the multiplied signals keeps degrading with increasing oscillation frequency.

As an alternative, one may shift to a hybrid approach, which converts the electrical signals to modulated optical signals and use the extremely low-loss optical fibers to store them. By doing this, the resonator can be effectively extended while the propagation loss is dramatically reduced, which leads to a very high Q factor. In addition, as the corresponding modulation and detection elements in the multi-gigahertz range are mature, it becomes the most ideal candidate for generating highly pure RF signals from hundreds of megahertz up to 100 GHz. This is the basic idea of an optoelectronic oscillator (OEO).[3–5] In the past few decades, remarkable developments of OEO systems have been achieved regarding single mode operation[6–9] and tunability with microwave photonic filters (MPFs).[10–17] However, most of the reported OEOs are implemented based on kilometer length fiber coils and a number of discrete optical components, which may limit their use in practical applications where a highly compact formfactor with low power consumption is desired.[3,18]

One reported solution for miniaturizing the system is to use a high-Q resonator formed by crystalline electro-optic (EO) materials to simultaneously serve as energy storage element, narrow bandwidth filter, and modulator.[3,19] However, it still includes discrete components and is challenging to realize mass production. At the same time, with the rapid development of photonic integrated circuits (PICs), several integrated OEOs[18,20,21] have been reported in recent years. These OEOs use either phase modulators or Mach–Zehnder interferometer (MZI)-based amplitude modulators, which also tend to require long interaction length (millimeter level). This may result in greater insertion loss and driving power.[22,23] In order to further reduce the footprint and the power consumption, resonant structure-based

modulators become attractive. One representative and extensively studied type is silicon microring modulators[22–27] leveraging the distinct complementary metal-oxide-semiconductor (CMOS) compatibility of silicon photonics. Building of an OEO with such modulators is rarely reported. In addition, will the relatively high Q factor of the included resonator help to improve the Q factor of the entire OEO loop and, thus, assist for the generation of low noise signals remains unknown.

In this work, a silicon microring resonator-based modulator working in the C band is presented. It has a large 3 dB bandwidth of ~31.7 GHz, which is appropriate for generating RF signals at multi-GHz. An OEO system based on this ring modulator is built up, and a 10 GHz RF signal with phase noise of nearly −90 dBc/Hz at 10 kHz offset is generated.

The silicon microring modulator used here is fabricated on a standard silicon-on-insulator (SOI) wafer with a 220 nm silicon device layer and a 2 μm buried oxide (BOX) via a CMOS process line. Figure 1 gives a microscope image of one fabricated modulator. It is implemented in a symmetrical add-drop configuration, which makes the device operate in slightly under-coupled state. A partially etched rib waveguide was used in the ring and bus coupling region with etch depth of 135 nm and waveguide width of 450 nm. The radius of the ring resonator is 10 μm, resulting in a large free spectral range (FSR) of 9.82 nm at zero bias as shown in Fig. 2(a), which is the normalized transmission at the output port. This large FSR can be potentially applied in coarse wavelength division multiplexing (CWDM) applications.

To apply the plasma dispersion effect for effective index change, the ring resonator was doped into a lateral p–n configuration. The modulator is operated in the carrier depletion mode, which means a reverse bias will be applied to the ring resonator. This mode avoids the speed limitation posed by the minority carrier lifetime as in the carrier injection mode.[22] When a voltage is applied, the effective index changes to produce a resonance shift of the ring ($\Delta\lambda$), as shown in Fig. 2(b), which is the normalized transmission at different reverse bias voltages. At a specific working wavelength, this ring resonance shift produces a power modulation at the bus output.

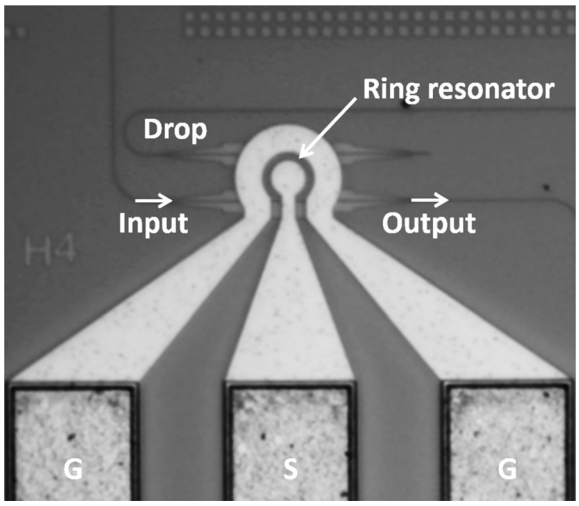

FIG. 1. Microscope image of the silicon microring modulator.

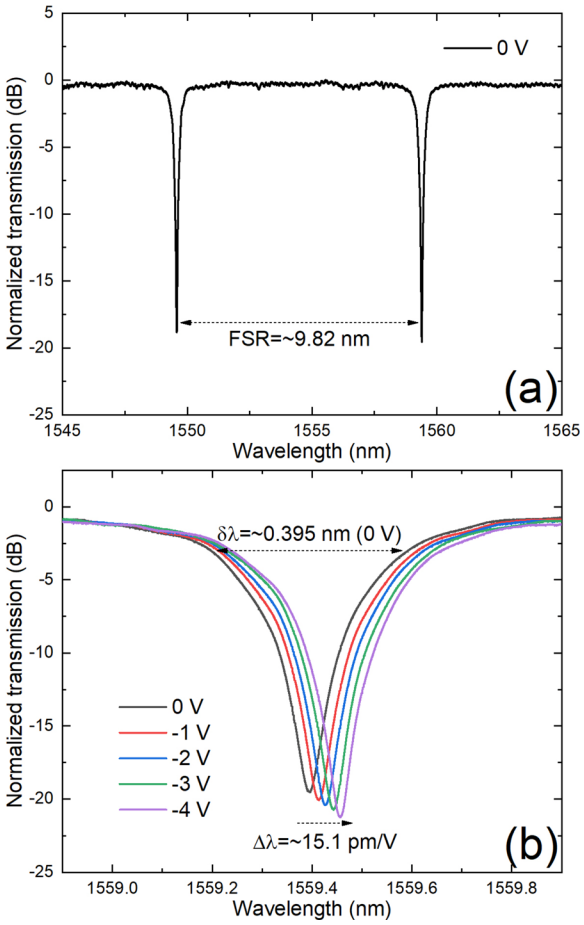

FIG. 2. (a) Normalized transmission spectrum of the ring modulator at 0 V indicating the ring FSR. (b) Enlarged transmission spectra at different bias voltages indicating the resonance shift and the width of the resonance at 0 V.

To achieve large extinction ratio (ER) with small insertion loss (IL), one should maximize the ratio of the ring resonance shift ($\Delta\lambda$) to the width of this resonance ($\delta\lambda$).[28] On the one hand, a high doping concentration should be employed to increase the index change, thus $\Delta\lambda$. However, this also causes a decrease in the intrinsic Q factor of the ring resonator due to higher propagation loss. Full width at half maximum (FWHM) of the ring resonance ($\delta\lambda$) may also be increased as a result. In addition, a higher doping concentration will lead to a larger junction capacitance, which may limit the device speed.[28] On the other hand, a small $\delta\lambda$ is favorable, which is equal to a large overall (loaded) Q factor. To do this, one should lower the doping concentration or increase the gap between the bus and the ring. However, a too large Q factor is also not desired as the photon lifetime-limited modulation bandwidth drops as a result of this.[28] In addition, when the Q factor becomes large, the intra ring power density increases, and nonlinear absorption may be induced as a result.[29,30]

In consideration of these factors, doping concentration in the ring resonator was targeted at $\sim 5 \times 10^{17}$ cm^{-3}, and no offset was applied to the location of the p and n regions. An optimal gap of 240 nm was selected, resulting in a power coupling coefficient of

~0.134. The transmission spectra shown in Fig. 2(b) are just from the modulator with the above parameters. $\delta\lambda$ at 0 V is 0.398 nm, corresponding to an overall Q factor of ~3950. Based on the equation $f = 1/2\pi\tau = c/\lambda Q$, which provides an estimate of the frequency limitation (f) due to the cavity photon lifetime (τ), this Q factor corresponds to a bandwidth limitation of 48.7 GHz. Wavelength shift ($\Delta\lambda$) in this bias range is ~15.1 pm/V. Then, the voltage required to induce a phase change of π (V_π) can be determined, and, thus, the corresponding modulation efficiency ($V_\pi L$) is calculated as $V_\pi L = L \cdot \mathrm{FSR}/2\Delta\lambda = 2.04$ V·cm, where L denotes the length of the p–n shifter.

To deepen the analysis of the DC characteristics, IL, ER, and transmitter penalty (TP) of the ring modulator for voltage swing from 0 to −4 V (4 V_{pp}) have been calculated from the data in Fig. 2(b) and shown in Fig. 3. Here IL is defined as the loss at the "1" level as compared to the input power to the device, which excludes the ~1.6 dB/facet edge coupler loss. ER refers to the power difference between the "1" and "0" levels. As shown in the figure, the modulator demonstrates a maximum ER of 11.7 dB with an IL of 9.2 dB.

A better figure-of-merit for optical modulators, which represents the best combination of IL and ER, is the transmitter penalty (TP).[31] It is defined as

$$TP = -10\log_{10}\left(\frac{P_1 - P_0}{2P_{in}}\right), \quad (1)$$

where P_1 and P_0 are optical powers at the "1" and "0" levels, respectively, and P_{in} is the input power to the modulator. TP results of the tested modulator for 4 V_{pp} are also shown in Fig. 3. A minimum value of 9.8 dB occurs at ~1559.55 nm, which corresponds to approximate the −6 dB point in the right half of the ring resonant peak. The following characterizations of the ring modulator were all conducted around this wavelength. The corresponding IL and ER are with moderate values of 4.2 and 3.4 dB, respectively. It is also noticeable that there is an asymmetry in TP. This is related to the changes in the transmission spectrum as a function of bias voltage shown in Fig. 2(b). To be specific, as the reverse bias voltage increases from 0 to −4 V, carriers are extracted from the ring area. As a result, the light propagation loss in the ring becomes smaller, and the Q factor of the ring resonator increases. This is evident in Fig. 2(b) that the transmission spectrum at −4 V is not a simple shift of that at 0 V but has a narrower resonant peak.

To apply the modulator into an OEO system, its high-speed characteristics are critical. Figure 4 shows the small signal EO response (S21) of the ring modulator at −2 V measured using a light wave component analyzer (LCA) and a network analyzer (NA) with an input RF power of −5 dBm. The EO 3 dB bandwidth of the modulator is determined to be ~31.7 GHz. This is noticeably lower than the photon lifetime-limited bandwidth (~48.7 GHz), which indicates that RC characteristics of the device also play a comparable role.[28] On the other hand, this bandwidth is sufficient for multi-GHz RF signal generation in the following OEO test.

With all key parameters of the silicon microring modulator clearly characterized, an OEO system was built up based on it. Figure 5 illustrates the schematic of the experimental setup. The red and blue lines indicate the optical and electrical paths, respectively. Continuous wave (CW) light at 1559.55 nm from a tunable laser is coupled to the silicon modulator after a polarization controller (PC). With the modulator, electrical signals are applied onto the light and let the modulated light carry them, until the modulated light reaches a high-speed photodetector (PD) where it is converted back to electrical signals. Then, these outputs of the PD are filtered (with an RF filter operating at 10 GHz) and amplified (with an RF amplifier, 38 dB gain), and part of them are fed back to the modulator again (with a 50:50 RF power divider) to modulate the light with the rest as output signals. This feedback loop can generate self-sustained oscillations if their overall gains are larger than the losses.

Figure 6(a) shows one generated RF signal from this OEO loop. The signal is at 10 GHz determined by the RF filter with more than 60 dB signal to noise ratio. Its second and third harmonics at 20 and 30 GHz, respectively, are also clearly shown. Figure 6(b) gives the corresponding single-sideband (SSB) phase noise spectrum of this 10 GHz signal. The phase noise approaches −90 dBc/Hz at 10 kHz offset. It is worth mentioning that the lowest phase noises were also obtained

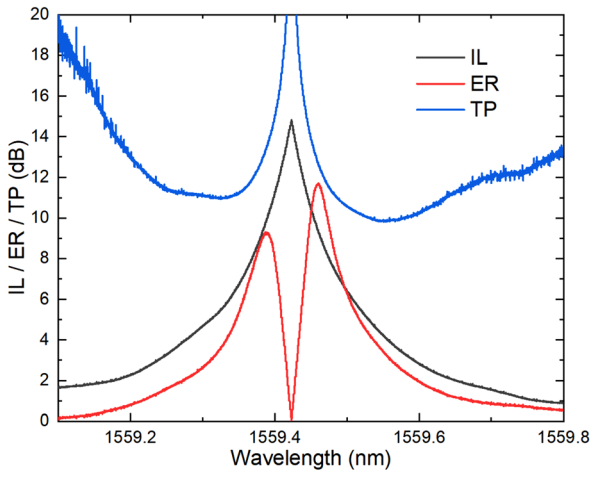

FIG. 3. Insertion loss (IL), extinction ratio (ER), and transmitter penalty (TP) of the ring modulator for voltage swing from 0 to −4 V.

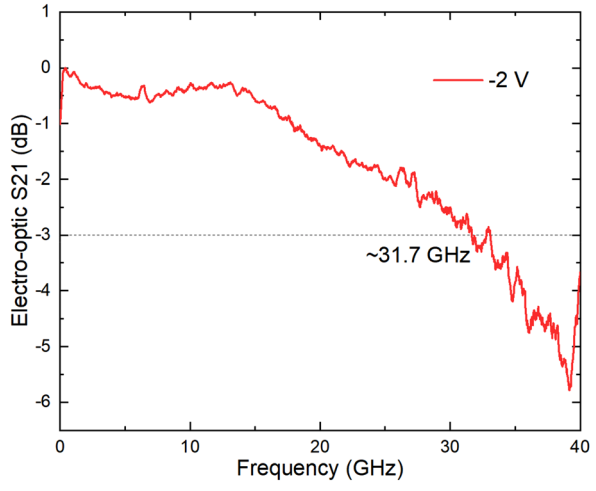

FIG. 4. Small signal EO response (S21) of the ring modulator at −2 V indicating a 3 dB bandwidth of ~31.7 GHz.

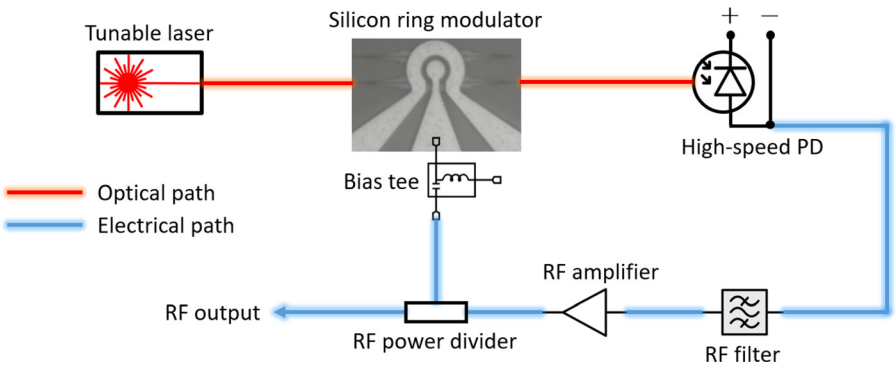

FIG. 5. Schematic of the experimental OEO setup. The red and blue lines indicate the optical and electrical paths, respectively.

around the wavelength corresponding to the minimum TP of the ring modulator.

This phase noise value is not as good as those of OEOs with fiber coils (kilometer length, phase noise from −102 dBc/Hz at 10 kHz offset[11] all the way to −163 dBc/Hz at 6 kHz offset[32]) or crystalline whispering gallery mode (WGM) disks (Q factor up to 10^{11}, phase noise approaching −110 dBc/Hz at 10 kHz offset[3]), which substantially extend the OEO loop delay. Here, the Q factor of the silicon microring resonator is limited to be at a moderate level and within a small range (10^3–10^4 level) due to the modulator design considerations mentioned earlier. This results that the resonator introduces a group delay of only several picoseconds at the output port,[33] which is much smaller than the fiber coil or crystalline WGM disk counterparts. It is known that the single-sideband phase noise of the generated RF signal can be expressed as[5]

$$S_{RF}(f') = \frac{\delta}{(\delta/2\tau_g)^2 + (2\pi)^2(\tau_g f')^2}, \tag{2}$$

where f' is the frequency offset from the OEO oscillation frequency, τ_g is the loop delay mainly introduced by the delay provides (optical fibers or high-Q resonators), and δ is the noise-to-signal ratio of the OEO and is defined as

$$\delta = \rho_N G_A^2 / P_{osc}, \tag{3}$$

where ρ_N is the total noise-density input to the oscillator and is the sum of the thermal noise, the shot noise, and the laser's relative-intensity noise (RIN), G_A is the voltage gain of the RF amplifier, and P_{osc} is the oscillation power. It is evident from Eq. (2) that, for fixed δ, the phase noise decreases quadratically with the loop delay time. This is the reason why OEO systems with kilometer-long fiber coils or ultrahigh-Q crystalline WGM disks have better noise performance. One possible solution to further improve the phase noise performance of integrated OEOs is to include an additional low-loss waveguide (with several cm length)[27,34,35] or a specially designed delay line based on cascaded ring resonators,[36,37] following the output of the modulator to increase the loop delay.

On the other hand, also because of including this relatively high-Q ring resonator and the group delay it brings in, the Q factor of the entire OEO loop is enhanced to be comparable to other integrated OEOs with larger mm footprint modulators. This is one of the reasons why the phase noise of this OEO system with microring modulator is at least on the same level with other reported integrated OEO systems.[18,20,21] Of course, the ultimate goal is to develop a fully integrated OEO system with all optical components on a chip, including integrated light sources, high-speed ring modulators, and PDs. All these components have been demonstrated in our previous work.[27,38–40]

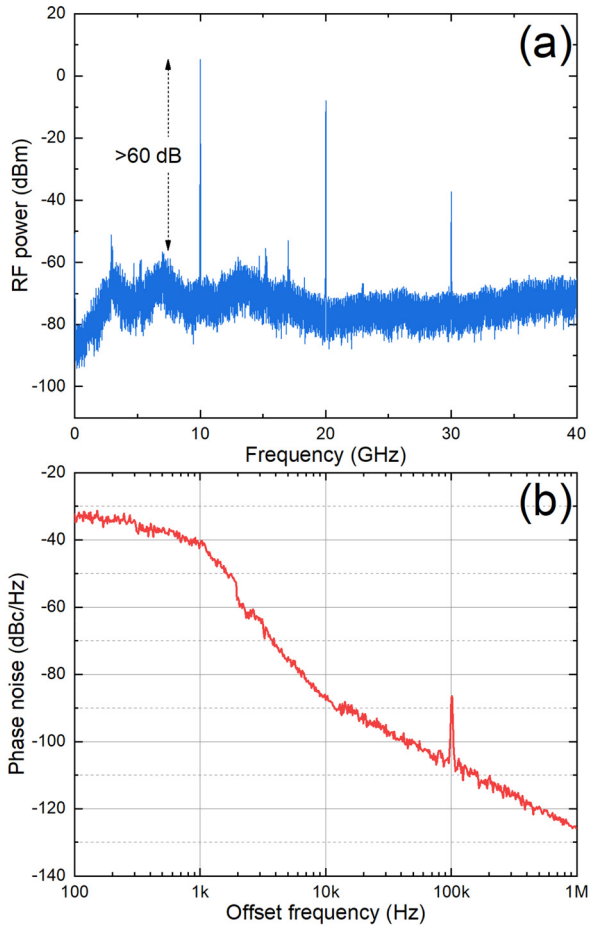

FIG. 6. (a) Electrical spectrum of one generated signal indicating a >60 dB signal to noise ratio at the fundamental 10 GHz. (b) Corresponding SSB phase noise spectrum of the 10 GHz signal.

In summary, an OEO system is built up with a high-speed silicon microring modulator. This modulator has a radius of 10 μm, a modulation efficiency ($V_\pi L$) of 2.04 V·cm, and an EO 3 dB bandwidth of 31.7 GHz. By using the modulator, this essential component of an OEO has been dramatically miniaturized even compared to other integrated OEOs. At the same time, assisted by the ring resonator, the phase noise of the generated 10 GHz signal (nearly −90 dBc/Hz at 10 kHz offset) is not compromised or even better compared to other integrated OEOs with mm footprint modulators. This work proves the feasibility and advantages of utilizing small footprint ring resonator-based silicon modulators in OEOs, which is an important step toward a compact, scalable, and fully integrated silicon photonics-based OEO system.

The authors would like to acknowledge the support from the Ministry of Education (MOE) Singapore (Grant No. MOE-T2EP50121-0005), Pinghu Laboratory Project (Grant No. 224120), Finance Science and Technology Project of Hainan Province (Grant No. ZDYF2020036), and the National Natural Science Foundation of China (Grant Nos. 62274048 and 61964007).

AUTHOR DECLARATIONS

Conflict of Interest

The authors have no conflicts to disclose.

Author Contributions

Xiang Li: Conceptualization (equal); Data curation (equal); Formal analysis (equal); Funding acquisition (lead); Investigation (equal); Methodology (equal); Visualization (lead); Writing – original draft (lead). **Jia Xu Brian Sia:** Data curation (equal); Formal analysis (equal); Investigation (equal); Methodology (equal); Writing – review & editing (equal). **Jiawei Wang:** Data curation (supporting); Formal analysis (supporting); Investigation (equal); Writing – review & editing (equal). **Zhongliang Qiao:** Funding acquisition (lead); Methodology (supporting); Supervision (supporting); Writing – review & editing (equal). **Wanjun Wang:** Methodology (equal); Writing – review & editing (equal). **Xin Guo:** Data curation (equal); Investigation (equal); Methodology (equal); Project administration (lead). **Hong Wang:** Conceptualization (equal); Formal analysis (equal); Funding acquisition (equal); Supervision (equal); Writing – review & editing (equal). **Chongyang Liu:** Conceptualization (equal); Formal analysis (equal); Funding acquisition (equal); Supervision (equal); Writing – review & editing (equal).

DATA AVAILABILITY

The data that support the findings of this study are available from the corresponding authors upon reasonable request.

REFERENCES

[1]A. Liu, J. Dai, and K. Xu, "Stable and low-spurs optoelectronic oscillators: A review," Appl. Sci. **8**, 2623 (2018).
[2]M. Li, T. Hao, W. Li, and Y. Dai, "Tutorial on optoelectronic oscillators," APL Photonics **6**, 061101 (2021).
[3]L. Maleki, "The optoelectronic oscillator," Nat. Photonics **5**, 728–730 (2011).
[4]X. S. Yao and L. Maleki, "Optoelectronic microwave oscillator," J. Opt. Soc. Am. B **13**, 1725–1735 (1996).
[5]X. S. Yao and L. Maleki, "Optoelectronic oscillator for photonic systems," IEEE J. Quantum Electron. **32**, 1141–1149 (1996).
[6]X. S. Yao, L. Maleki, Y. Ji, G. Lutes, and M. Tu, "Dual-loop opto-electronic oscillator," in *Proceedings of the IEEE International Frequency Control Symposium (FCS '98)* (IEEE 1998), pp. 545–549.
[7]X. S. Yao, L. Davis, and L. Maleki, "Coupled optoelectronic oscillators for generating both RF signal and optical pulses," J. Lightwave Technol. **18**, 73–78 (2000).
[8]W. Zhou and G. Blasche, "Injection-locked dual opto-electronic oscillator with ultra-low phase noise and ultra-low spurious level," IEEE Trans. Microwave Theory Tech. **53**, 929–933 (2005).
[9]J. Zhang and J. Yao, "Parity-time-symmetric optoelectronic oscillator," Sci. Adv. **4**, eaar6782 (2018).
[10]X. Xie, C. Zhang, T. Sun, P. Guo, X. Zhu, L. Zhu, W. Hu, and Z. Chen, "Wideband tunable optoelectronic oscillator based on a phase modulator and a tunable optical filter," Opt. Lett. **38**, 655–657 (2013).
[11]W. Li and J. Yao, "A wideband frequency tunable optoelectronic oscillator incorporating a tunable microwave photonic filter based on phase-modulation to intensity-modulation conversion using a phase-shifted fiber Bragg grating," IEEE Trans. Microwave Theory Techn. **60**, 1735–1742 (2012).
[12]Z. Tang, S. Pan, D. Zhu, R. Guo, Y. Zhao, M. Pan, D. Ben, and J. Yao, "Tunable optoelectronic oscillator based on a polarization modulator and a chirped FBG," IEEE Photonics Technol. Lett. **24**, 1487–1489 (2012).
[13]S. Pan and J. Yao, "Wideband and frequency-tunable microwave generation using an optoelectronic oscillator incorporating a Fabry-Perot laser diode with external optical injection," Opt. Lett. **35**, 1911–1913 (2010).
[14]M. Li, W. Li, and J. Yao, "Tunable optoelectronic oscillator incorporating a high-Q spectrum-sliced photonic microwave transversal filter," IEEE Photonics Technol. Lett. **24**, 1251–1253 (2012).
[15]F. Jiang, J. H. Wong, H. Q. Lam, J. Zhou, S. Aditya, P. H. Lim, K. E. K. Lee, P. P. Shum, and X. Zhang, "An optically tunable wideband optoelectronic oscillator based on a bandpass microwave photonic filter," Opt. Express **21**, 16381–16389 (2013).
[16]H. Peng, C. Zhang, X. Xie, T. Sun, P. Guo, X. Zhu, L. Zhu, W. Hu, and Z. Chen, "Tunable DC-60 GHz RF generation utilizing a dual-loop optoelectronic oscillator based on stimulated Brillouin scattering," J. Lightwave Technol. **33**, 2707–2715 (2015).
[17]M. Shi, L. Yi, W. Wei, and W. Hu, "Generation and phase noise analysis of a wide optoelectronic oscillator with ultra-high resolution based on stimulated Brillouin scattering," Opt. Express **26**, 16113–16124 (2018).
[18]W. Zhang and J. Yao, "Silicon photonic integrated optoelectronic oscillator for frequency-tunable microwave generation," J. Lightwave Technol. **36**, 4655–4663 (2018).
[19]L. Maleki, "The opto-electronic oscillator (OEO): review and recent progress," in *European Frequency and Time Forum* (IEEE, Gothenburg, Sweden, 2012), pp. 497–500.
[20]P. T. Do, C. Alonso-Ramos, X. Le Roux, I. Ledoux, B. Journet, and E. Cassan, "Wideband tunable microwave signal generation in a silicon-micro-ring-based optoelectronic oscillator," Sci. Rep. **10**, 6982 (2020).
[21]M. Merklein, B. Stiller, I. V. Kabakova, U. S. Mutugala, K. Vu, S. J. Madden, B. J. Eggleton, and R. Slavík, "Widely tunable, low phase noise microwave source based on a photonic chip," Opt. Lett. **41**, 4633–4636 (2016).
[22]G. T. Reed, G. Mashanovich, F. Y. Gardes, and D. J. Thomson, "Silicon optical modulators," Nat. Photonics **4**, 518–526 (2010).
[23]P. Dong, S. Liao, D. Feng, H. Liang, D. Zheng, R. Shafiiha, C.-C. Kung, W. Qian, G. Li, X. Zheng, A. V. Krishnamoorthy, and M. Asghari, "Low V_{pp}, ultralow-energy, compact, high-speed silicon electro-optic modulator," Opt. Express **17**, 22484–22490 (2009).
[24]Q. Xu, B. Schmidt, S. Pradhan, and M. Lipson, "Micrometre-scale silicon electro-optic modulator," Nature **435**, 325–327 (2005).
[25]M. Pantouvaki, P. Verheyen, J. D. Coster, G. Lepage, P. Absil, and J. Van Campenhout, "56Gb/s ring modulator on a 300 mm silicon photonics platform," in *Proceedings of IEEE European Conference on Optical Communications* (IEEE 2015).
[26]T. Baba, S. Akiyama, M. Imai, N. Hirayama, H. Takahashi, Y. Noguchi, T. Horikawa, and T. Usuki, "50-Gb/s ring-resonator-based silicon modulator," Opt. Express **21**, 11869–11876 (2013).

[27]J. X. B. Sia, X. Li, J. Wang, W. Wang, Z. Qiao, X. Guo, C. W. Lee, A. Sasidharan, S. Gunasagar, C. G. Littlejohns, C. Liu, G. T. Reed, K. S. Ang, and H. Wang, "Wafer-scale demonstration of low-loss (∼0.43 dB/cm), high-bandwidth (>38 GHz), silicon photonics platform operating at the C-band," IEEE Photonics J. **14**, 1–9 (2022).
[28]G. Li, A. V. Krishnamoorthy, I. Shubin, J. Yao, Y. Luo, H. Thacker, X. Zheng, K. Raj, and J. E. Cunningham, "Ring resonator modulators in silicon for interchip photonic links," IEEE J. Select. Top. Quantum Electron. **19**, 95–113 (2013).
[29]C. Xiang, W. Jin, J. Guo, C. Williams, A. M. Netherton, L. Chang, P. A. Morton, and J. E. Bowers, "Effects of nonlinear loss in high-Q Si ring resonators for narrow-linewidth III-V/Si heterogeneously integrated tunable lasers," Opt. Express **28**, 19926–19936 (2020).
[30]M. Borselli, T. J. Johnson, and O. Painter, "Beyond the Rayleigh scattering limit in high-Q silicon microdisks: Theory and experiment," Opt. Express **13**, 1515–1530 (2005).
[31]M. Pantouvaki, P. Verheyen, G. Lepage, J. De Coster, H. Yu, P. De Heyn, P. Absil, and J. Van Campenhout, "20Gb/s silicon ring modulator co-integrated with a Ge monitor photodetector," in 39th European Conference and Exhibition on Optical Communication (ECOC 2013), 2013.
[32]D. Eliyahu, D. Seidel, and L. Maleki, "Phase noise of a high performance OEO and an ultra low noise floor cross-correlation microwave photonic homodyne system," in *IEEE International Frequency Control Symposium* (IEEE 2008), pp. 811–814.
[33]O. Schwelb, "Transmission, group delay, and dispersion in single-ring optical resonators and add/drop filters-a tutorial overview," J. Lightwave Technol. **22**, 1380–1394 (2004).
[34]W. Bogaerts and S. K. Selvaraja, "Compact single-mode silicon hybrid rib/strip waveguide with adiabatic bends," IEEE Photonics J. **3**, 422–432 (2011).
[35]P. Dong, W. Qian, S. Liao, H. Liang, C.-C. Kung, N.-N. Feng, R. Shafiiha, J. Fong, D. Feng, A. V. Krishnamoorthy, and M. Asghari, "Low loss shallow-ridge silicon waveguides," Opt. Express **18**, 14474–14479 (2010).
[36]M. Burla, D. Marpaung, L. Zhuang, C. Roeloffzen, M. R. Khan, A. Leinse, M. Hoekman, and R. Heideman, "On-chip CMOS compatible reconfigurable optical delay line with separate carrier tuning for microwave photonic signal processing," Opt. Express **19**, 21475–21484 (2011).
[37]J. Cardenas, M. A. Foster, N. Sherwood-Droz, C. B. Poitras, H. L. Lira, B. Zhang, A. L. Gaeta, J. B. Khurgin, P. Morton, and M. Lipson, "Wide-bandwidth continuously tunable optical delay line using silicon microring resonators," Opt. Express **18**, 26525–26534 (2010).
[38]J. X. B. Sia, X. Li, W. Wang, Z. Qiao, X. Guo, J. Zhou, C. G. Littlejohns, C. Liu, G. T. Reed, and H. Wang, "Sub-kHz linewidth, hybrid III-V/silicon wavelength-tunable laser diode operating at the application-rich 1647–1690 nm," Opt. Express **28**, 25215–25224 (2020).
[39]J. X. B. Sia, W. Wang, Z. Qiao, X. Li, X. Guo, J. Zhou, C. G. Littlejohns, Z. Zhang, C. Liu, G. T. Reed, and H. Wang, "Compact silicon photonic hybrid ring external cavity (SHREC)/InGaSb-AlGaAsSb wavelength-tunable laser diode operating from 1881–1947 nm," Opt. Express **28**, 5134–5146 (2020).
[40]X. Li, J. X. B. Sia, W. Wang, Z. Qiao, X. Guo, G. I. Ng, Y. Zhang, Z. Niu, C. Tong, H. Wang, and C. Liu, "Phase noise reduction of a 2 μm passively mode-locked laser through hybrid III-V/silicon integration," Optica **8**, 855–860 (2021).